ANTIOXIDANTS & REDOX SIGNALING
Volume 14, Number 1, 2011
© Mary Ann Liebert, Inc.
DOI: 10.1089/ars.2010.3458

Improving the Stability of α-Conotoxin AuIB Through N-to-C Cyclization: The Effect of Linker Length on Stability and Activity at Nicotinic Acetylcholine Receptors

Christopher J. Armishaw,[1,2] Anders A. Jensen,[2] Lena D. Balle,[2] Krystle C.M. Scott,[1] Lena Sørensen,[2] and Kristian Strømgaard[2]

Abstract

Modification of α-conotoxin frameworks through cyclization *via* an oligopeptide linker has previously been shown as an effective strategy for improving *in vivo* stability. We have extended this strategy by investigating cyclic analogs of α-conotoxin AuIB, a selective $\alpha_3\beta_4$ nicotinic acetylcholine receptor (nAChR) antagonist, to examine a range of oligopeptide linker lengths on the oxidative formation of disulfide bonds, activity at nAChRs, and stability to degradation by chymotrypsin. Upon nondirected random oxidation, the ribbon isomer formed preferentially with the globular isomer occurring as a minor by-product. Therefore, a regioselective disulfide bond forming strategy was used to prepare the cAuIB-2 globular isomer in high yield and purity. The cAuIB-2 globular isomer exhibited a threefold decrease in activity for the $\alpha_3\beta_4$ nAChR compared to wild-type-AuIB, although it was selective for $\alpha_3\beta_4$ over α_7 and $\alpha_4\beta_2$ subtypes. On the other hand, the cAuIB-2 ribbon isomer was shown to be inactive at all three nAChR subtypes. Nonetheless, all of the cyclic analogs were found to be significantly more stable to degradation by chymotrypsin than wild-type AuIB. As such, the cAuIB-2 globular isomer could constitute a useful probe for studying the role of the $\alpha_3\beta_4$ nAChR in a range of *in vivo* experimental paradigms. *Antioxid. Redox Signal.* 14, 65–76.

Introduction

Venomous marine cone snails use their venom to disrupt the essential functions of the central and peripheral nervous system to facilitate prey capture or for self-defense (40). Their venom is composed of a complex mixture of disulfide-rich peptide neurotoxins known as conotoxins that selectively target a large variety of membrane proteins in both the central and peripheral nervous systems (4, 45). The high degree of selectivity displayed by individual neurotoxins in these venoms for a specific molecular target makes them excellent tools for studying the roles of specific membrane proteins for neurotransmission and provides a source of ligands that are often potent and highly selective for different classes of ion channels, receptors, and transporters (29). In recent years conotoxins have been under investigation for the treatment of many neuropathological conditions, including chronic neuropathic pain, diabetes, multiple sclerosis, and cardiovascular disease (30). This has led to the approval of the first conotoxin drug, Prialt (ω-conotoxin MVIIA) by the U.S. Food and Drug Administration as an analgesic (39), with a number of other conotoxins currently undergoing clinical or preclinical development (12, 32, 33).

The α-conotoxins are a class of conotoxins that demonstrate unique selectivities for different subtypes of nicotinic acetylcholine receptors (nAChRs) (3). nAChRs are ligand-gated pentameric ion channels constructed from five subunits. To date, 17 nAChR subunits have been cloned and are defined as α_1-α_{10}, β_1-β_4, δ-, γ-, and ε-subunits (36). Acetylcholine-mediated activations of receptors assembled by these subunits produces fast synaptic neurotransmission and modulates the release of additional neurotransmitters. Muscle-type nAChRs are composed of α_1, β_1, δ-, γ-, and ε-subunits, whereas neuronal nAChRs are composed of any homo- or heteromeric combination of five α_2-α_{10} and β_2-β_4 subunits (25). The $\alpha_4\beta_2$, $\alpha_3\beta_4$, and α_7 nAChRs are the predominant subtypes expressed in mammalian brain; however, a large number of other subunit combinations and stoichiometric ratios for neuronal nAChRs are available, thus underlining the therapeutic importance of developing subtype specific ligands for these receptors (44).

[1]Torrey Pines Institute for Molecular Studies, Port St. Lucie, Florida.
[2]Department of Medicinal Chemistry, Faculty of Pharmaceutical Sciences, University of Copenhagen, Copenhagen, Denmark.

Although small in size (12–20 amino acids), α-conotoxins exhibit well-defined three-dimensional structures characterized by a 3_{10}-helical barrel that projects residues into the orthosteric binding site of the nAChR (38). Their highly rigid structural frameworks can be attributed to the presence of two highly conserved disulfide bonds that exist in a Cys^{I}-Cys^{III} and Cys^{II}-Cys^{IV} (globular) arrangement (Fig. 1A). This gives rise to a framework of two intervening loops of hypervariable amino acids denoted *m* and *n*, respectively (19). The majority of α-conotoxins characterized to date that target neuronal nAChRs possess a 4/7 loop framework, although others continue to be characterized including 4/6 (AuIB), 4/4 (BuIA), and 4/3 (ImI, ImII, and RgIA) (8) (Fig. 2). In addition to the globular disulfide bond isomer, there are two other possible disulfide bond arrangements that can form, defined as the Cys^{I}-Cys^{IV}, Cys^{II}-Cys^{III} (ribbon), and Cys^{I}-Cys^{II}, Cys^{III}-Cys^{IV} (beads) isomers (Fig. 1A). Engineering α-conotoxins with these non-native arrangements results in analogs with very different structural and pharmacological properties (18, 21, 41).

α-Conotoxin AuIB is the only α-conotoxin identified to date that possesses the 4/6 loop framework. Structurally, AuIB resembles other α-conotoxins that possess the 4/7 loop framework (Fig. 2) (10). AuIB is a specific antagonist of the neuronal $\alpha_3\beta_4$ nAChR, making it a useful tool for probing the physiological functions maintained by this nAChR subtype (37). Antagonists of $\alpha_3\beta_4$ nAChRs have been shown to decrease nicotine self-administration in rats, suggesting that this receptor is also a potential target for treating nicotine dependence (23, 43). As such, the discovery of new $\alpha_3\beta_4$ nAChR antagonists could have profound implications as *in vivo* research tools in the development of novel smoking cessation treatments.

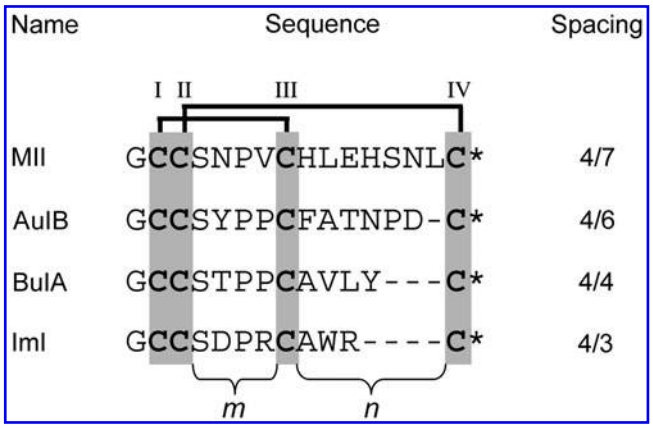

FIG. 2. Sequences of α-conotoxins with different spacing in their respective *n*-loops. Cysteine residues are labeled 1–4, respectively, and native disulfide bond connectivity is indicated. The *asterisk* denotes a C-terminal carboxamide.

AuIB blocks nicotine-stimulated hippocampal norepinephrine release but not striatal dopamine release, demonstrating that AuIB is able to discriminate among different native nAChR subtypes (37). Further, the ribbon isomer of AuIB has been found to be 10-fold more active for the $\alpha_3\beta_4$ nAChR than the native globular isomer (18), although it has also been reported that significant differences in activity between the two isomers exist between native and oocyte-expressed $\alpha_3\beta_4$ receptors (41). The ribbon isomer exhibited reduced structural definition when compared with the globular isomer (Fig. 1B, C). As such, observed differences in

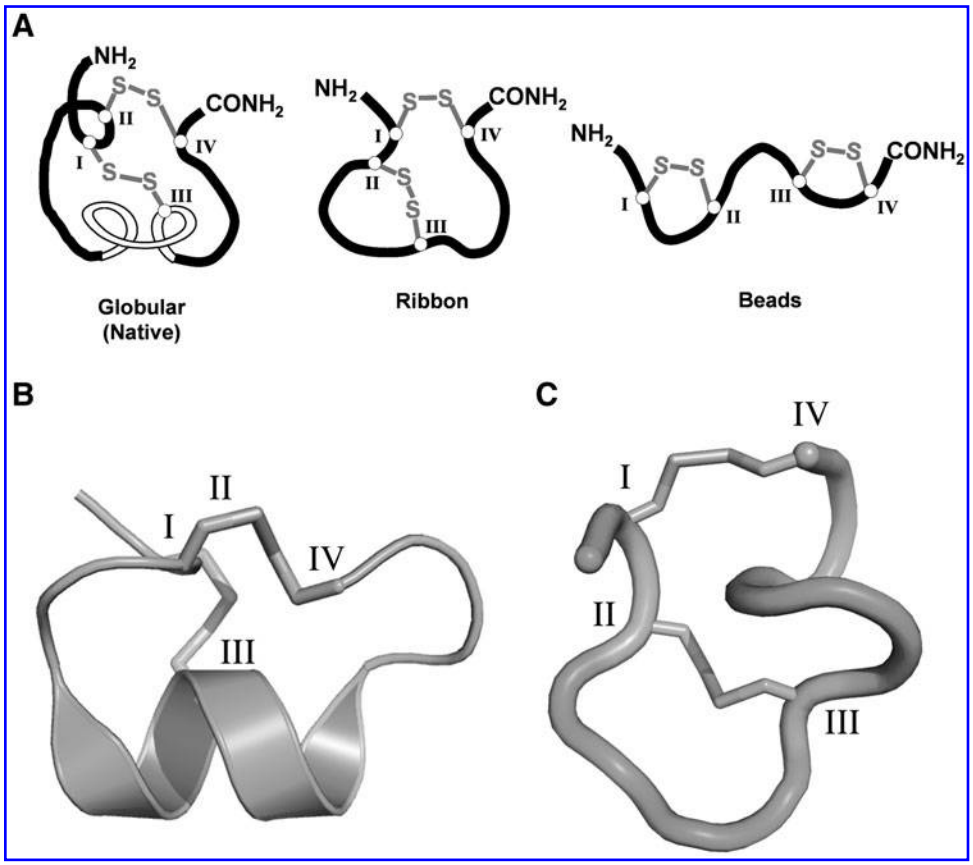

FIG. 1. Structures of α-conotoxin disulfide bond isomers. (A) Three possible disulfide bond isomers of an α-conotoxin; nuclear magnetic resonance solution structures of **(B)** α-conotoxin AuIB globular (PDB ID: 1MXN) and **(C)** ribbon isomer (PDB ID: 1MXP). Disulfide bonds are shown with cysteine numbering indicated in Roman numerals.

pharmacological activity can be attributed to the increased flexibility of the ribbon isomer, which would be more readily able to adopt the biologically active conformation upon receptor binding (18).

Despite their potential as drug candidates and their application as important pharmacological tools, α-conotoxins like many other classes of peptides exhibit poor *in vivo* stability and short half-lives as a result of their inherent vulnerability to enzymatic degradation, limiting their potential for use in *in vivo* experiments and as drug candidates (31). Moreover, while conotoxins contain multiple disulfide bonds that restrict their conformation, the disulfide bonds themselves are not entirely stable in the presence of physiological reducing agents such as glutathione and serum albumin (5). N-to-C cyclization of peptides is one method commonly used to stabilize the conformation of many classes of peptides in solution to enhance their *in vivo* stability (1, 22, 28). Further, there is a growing interest in a class of peptides known as cyclotides, which possess multiple disulfide bonds in addition to their circular backbone that exhibit phenomenal stability under a variety of stress conditions (13, 14).

In view of the superior stability of cyclic peptides over linear peptides, N-to-C cyclization of α-conotoxins is a feasible approach to improve their *in vivo* stability, a principle that has been demonstrated previously with the synthesis of cyclic α-conotoxin MII and χ-conotoxin MrIA analogs (11, 34). In these studies, the cyclic conotoxin analogs were found to possess greater resistance to proteolysis, as well as enhanced stability in human plasma, yet the analogs retained the biological activity and the three dimensional conformations when compared to the native conotoxin. It was recently reported that N-to-C cyclization of α-conotoxin ImI through short oligopeptide linker units (1–3 amino acids) showed a clear preference for the formation of the non-native ribbon disulfide bond isomer (6). Although each of these studies was successful in producing α-conotoxin analogs with enhanced stability, a limited number of linker sizes were investigated (6, 11, 34).

In this report, we describe the synthesis, pharmacological characterization, and stability of a series of N-to-C cyclic analogs of α4/6-conotoxin AuIB. Given that the ribbon isomer of α-conotoxin AuIB displays a higher antagonistic potency for $\alpha_3\beta_4$ nAChRs (18), we reasoned that N-to-C cyclization through short oligopeptide linker units would result in the spontaneous formation of the ribbon isomer and could possibly lead to $\alpha_3\beta_4$ nAChR antagonists with enhanced *in vivo* stability. In comparison to previous studies concerning cyclized conotoxin analogs (6, 11, 34), our study investigates a wider range of linker lengths of between one and seven amino acid residues, and assesses their influence on the formation of disulfide bond isomers, *in vitro* stability and biological activity. In a complementary study, Lovelace *et al.* also synthesized a series of cAuIB derivatives, which focused on linkers of 4–7 amino acid residues, with additional structural characterization by nuclear magnetic resonance (NMR) spectroscopy (35). The findings of their study are broadly consistent with those reported in this article.

Materials and Methods

Chemistry

Materials. Reagents and materials were purchased from commercial suppliers and used without further purification. Protected amino acid derivatives and 4-methylbenzhydrylamine (MBHA) resin were purchased from ChemImpex (Wood Dale, IL) and *S*-tritylmercaptopropyl MBHA resin from Peptides International (Louisville, KY). 2-(1*H*-benzotriazol-1-yl)-1,1,3,3-tetramethyluronium hexafluorophosphate was purchased from ChemPep (Miami, FL).

Liquid chromatography mass spectrometry analysis. Liquid chromatography mass spectrometry (LC-MS) spectra were recorded using a Shimadzu 2010EV liquid chromatography mass spectrometry system (Kyoto, Japan) equipped with a photo diode array detector. A Phenomenex Jupiter column (C_{18}, 5×0.46 cmID, 5 μm) (Torrance, CA) was used to achieve analytical separations. Gradients of 10% aqueous MeCN + 0.05% formic acid (buffer A) and 90% aqueous MeCN + 0.046% formic acid (buffer B) were employed. Preparative reversed phase high performance liquid chromatography (RP-HPLC) was performed using a Shimadzu LC8A preparative system. A Phenomenex Luna preparative RP-HPLC column (C_{18}, 15×2.5 cmID, 10 μm) was used to achieve chromatographic separations. Gradients of 10% aqueous MeCN + 0.5% trifluoroacetic acid (TFA) (buffer A) and 90% aqueous MeCN + 0.5% TFA (buffer B) were employed.

LC-MS/MS spectra were recorded using Agilent 1200 series solvent delivery system equipped with an auto injector coupled to an Agilent 6410 triple quadrupole mass spectrometer equipped with an electrospray ionization source. Gradients of 10% aqueous acetonitrile + 0.05% formic acid (buffer A) and 90% aqueous acetonitrile + 0.046% formic acid (buffer B) were employed with a flow rate of 0.75 ml/min. A Zorbax column (C_{18} column, 2.1×0.50 cmID, 2 μm) was used.

Peptide synthesis. All peptides were assembled in parallel using the tea bag methodology as previously described (24), employing 2-(1*H*-benzotriazol-1-yl)-1,1,3,3-tetramethyluronium hexafluorophosphate activation of N^{α}-*tert*-butyloxycarbonyl protected amino acids with *in situ* neutralization chemistry (42). The following amino acid protecting groups were used: Cys, 4-methylbenzyl; Asp, O-cyclohexyl; Asn, xanthyl; Thr, benzyl; Tyr, 2-bromobenzyloxycarbonyl; Ser, benzyl. The directed disulfide bond synthesis of cAuIB-2 utilized acetomidomethyl (Acm) protection at positions Cys2 and Cys7 for the globular isomer, or Cys2 and Cys14 for the ribbon isomer in the linear thioester precursor peptides. Native α-conotoxin AuIB and *Ac*-AuIB were assembled on MBHA resin, and thioester peptide precursors were assembled on *S*-tritylmercaptopropyl MBHA resin. The *N*-terminal of *Ac*-AuIB was acetylated using a mixture of acetic anhydride/diisopropylethylamine/dimethylformamide (1:1:8), (2×30 min) before cleavage. Cleavages were performed by treating each tea bag containing the peptide-resin with 5 ml of HF/*p*-cresol (9:1) (v/v) for 2 h at 0°C. After evaporation of the HF under a stream of nitrogen, the crude peptide thioesters were precipitated and washed with cold methyl-*tert*-butylether ether (2×10 ml), filtered, and lyophilized from 95% aqueous acetic acid and again from 50% aqueous acetonitrile + 0.1% TFA.

The crude linear reduced thioester peptides (30 mg) were shaken in aqueous 0.1 M phosphate buffer pH 8.2 (50 ml) in an open flask and the oxidations monitored by LC-MS analysis to ensure reaction completion. The mixtures were acidified to

pH 2 with TFA and each peak was isolated to >95% purity by preparative RP-HPLC. The second disulfide bond in cAuIB-2 was formed by treating the partially protected/oxidized cyclic peptide (10 mg) in 10 m*M* HCl containing 80% aqueous methanol (25 ml) with ~10 equivalents of I_2 per Acm group. The mixture was stirred for 5 min under an inert N_2 atmosphere and the reaction quenched by drop-wise addition of 0.1M $Na_2O_3S_2$ until colorless. The fully oxidized peptide was loaded onto a preparative RP-HPLC column by direct infusion and eluted and fractionated accordingly using a linear gradient to >95% purity.

Circular dichroism (CD) spectra were recorded on a Jasco J-720 spectropolarimeter (Easton, MD) at ambient temperature in the low UV range (190–260 nm) using a quartz cell with a 1-mm path length. Samples were dissolved in 50 m*M* phosphate buffer, pH 7.2 at a concentration of 30 μM. Each spectrum represents an average of 5 scans (scan speed 50 nm/min).

Disulfide bond determination. A modified reduction/alkylation strategy based on the method of Clark *et al.* was used to determine the disulfide bond connectivity of cAuIB-1 (11). Partial reduction was achieved by incubating the peptide (50 μg in 0.2M citrate buffer (pH 3, 50 μl) with 50 equivalents of *tris*-(2-carboxyethyl)phosphine hydrochloride (TCEP) at 25°C for 5 min, after which it was injected onto RP-HPLC and fractionated using a linear gradient. Fractions were analyzed by LC-MS and those containing the partially reduced conotoxin (+2 amu) were pooled, and an equal volume of 50 m*M* *N*-ethylmaleimide in *n*-propanol was added and incubated at 37°C for 1 h to alkylate the free thiol groups on cysteine residues. The partially reduced/alkylated conotoxin was then isolated by RP-HPLC and remaining disulfide bonds were reduced by treatment with 50 equivalents of TCEP in 0.2 M citrate overnight at 37°C, isolated by RP-HPLC, and lyophilized.

The reduced/alkylated/cyclic peptide was dissolved in 50 m*M* tris buffered to pH 7.4 (50 μl) and 1 μl of a solution of bovine pancreatic α-chymotrypsin (Sigma-Aldrich, St. Louis, MO) (1 mg/ml) dissolved in 50 m*M* tris buffered to pH 7.4 was added. The peptide was incubated overnight at 37°C and the reduced/alkylated/linear peptide was analyzed by LC-MS/MS to identify location of the two alkylated cysteine residues in the amino acid sequence.

Chymotrypsin stability assay. A solution containing the α-conotoxin AuIB analog in 50 m*M* tris buffer, pH 7.4 (0.5 μM), was prepared, together with a stock solution of chymotrypsin in 50 m*M* tris, pH 7.4 (1 mg/ml). Both solutions were pre-incubated to 37°C, before 5 μl of the chymotrypsin stock solution was added to 200 μl of each conotoxin analog stock solutions. About 20 μl aliquots were removed and quenched with 10 μl of 5% TFA/acetonitrile at successive time intervals. Stability experiments were performed in triplicate and each sample was analyzed by LC-MS. Percentage degradation was determined by measuring the ratio of the peak height of the proteolytically cleaved conotoxin and the residual conotoxin peak.

Pharmacology

Materials. Culture media, serum, antibiotics, and buffers for cell culture were obtained from Invitrogen (Paisley, United Kingdom). ACh was purchased from Sigma (St. Louis, MO) and epibatidine from Tocris (Bristol, United Kingdom). The r$\alpha_3\beta_4$-HEK293 (46), m$\alpha_4\beta_2$-HEK293T (27), and hα_7-GH3 cell lines (20) were generous gifts from Drs. Y. Xiao and K. Kellar (Georgetown University School of Medicine, Washington, DC), Dr. J.A. Stitzel (University of Colorado, Boulder, CO), and Dr. D. Feuerbach (Novartis Institutes of Biomedicinal Research, Basel, Switzerland), respectively.

Cell culture. The cell lines used in this study were cultured at 37°C in a humidified 5% CO_2 incubator. The cells were maintained in the culture medium (Dulbecco's modified Eagle's medium supplemented with penicillin [100 U/ml], streptomycin [100 μg/ml], and 10% fetal bovine serum). The r$\alpha_3\beta_4$-HEK293 cell line was maintained in the culture medium supplemented with 1 mg/ml G-418, the hα_7-GH3 cell line in the culture medium supplemented with 0.1 mg/ml G-418, and the m$\alpha_4\beta_2$-HEK293T cell line in the culture medium supplemented with 0.1 mg/ml zeozin and 0.5 mg/ml hygromycin.

Functional assays. The functional properties of the AuIB analogs as nAChR antagonists were characterized by using the Ca^{2+}/Fluo-4 assay for the hα_7-GH3 and r$\alpha_3\beta_4$-HEK293 cell lines and by using the FLIPR™ Membrane Potential (FMP) Blue assay for the m$\alpha_4\beta_2$-HEK293T cell line. The cells were split into poly-D-lysine-coated black 96-well plates with clear bottom (BD Biosciences, Palo Alto, CA), and the assay was performed 16–24 h later (r$\alpha_3\beta_4$-HEK293 and m$\alpha_4\beta_2$-HEK293T cell lines) or 64–72 h later (hα_7-GH3 cell line).

In the Ca^{2+}/Fluo-4 assay, the medium was aspirated and the cells were incubated in 50 μl loading buffer (Hank's buffered saline solution containing 20 m*M* HEPES, 1 m*M* $CaCl_2$, 1 m*M* $MgCl_2$, and 2.5 m*M* probenecid, pH 7.4, supplemented with 6 m*M* Fluo–4/AM [Molecular Probes, Eugene, OR]) at 37°C for 1 h. The loading buffer was aspirated, the cells were washed once with 100 μl assay buffer (Hank's buffered saline solution containing 20 m*M* HEPES, 1 m*M* $CaCl_2$, 1 m*M* $MgCl_2$, and 2.5 m*M* probenecid, pH 7.4), and then 100 μl assay buffer containing various concentrations of the AuIB analogs was added to the wells. For the experiments with α7-GH3 cell line, the assay buffer was supplemented with 100 μM genistein. After a 30 min incubation at 37°C in a humidified 5% CO_2 incubator, the 96-well plate was assayed in a NOVOstar™ microplate reader (BMG Labtechnologies, Offenburg, Germany) measuring emission (in fluorescence units) at 520 nm caused by excitation at 485 nm before and up to 60 s after addition of 33 μl agonist solution (the agonists were dissolved in assay buffer).

In the FMP assay, the medium was aspirated, and the cells were washed with 100 μl Krebs buffer (140 m*M* NaCl/4.7 m*M* KCl/2.5 m*M* $CaCl_2$/1.2 m*M* $MgCl_2$/11 m*M* HEPES/10 m*M* D-Glucose, pH 7.4). About 50 μl Krebs buffer containing various concentrations of α-conotoxin analogs was added to the wells and then an additional 50 μl Krebs buffer supplemented with 1.0 mg/ml FMP Blue dye (Molecular Devices, Crawley, United Kingdom) was added to each well. Then, the plate was incubated at 37°C in a humidified 5% CO_2 incubator for 30 min and assayed in the NOVOstar plate reader measuring emission (in fluorescence units) at 560 nm caused by excitation at 530 nm before and up to 1 min after addition of 33 μl ACh solution (ACh was dissolved in Krebs buffer). The

α-conotoxin analogs were characterized in duplicate at least three times at the three nAChR subtypes, and EC_{70}-EC_{90} agonist concentrations were used in the experiments (10 μM ACh for hα_7-GH3, 100 nM epibatidine for r$\alpha_3\beta_4$-HEK293, and 50 μM ACh for m$\alpha_4\beta_2$-HEK293T).

Results

Design and synthesis of analogs

A series of seven cyclic analogs of AuIB were synthesized by incorporating variable length peptide linker units consisting of one to seven amino acid residues to link the N- and C-termini to assess their impact on the random formation of disulfide bond isomers under oxidative condition, as well as their *in vitro* stability and nAChR activity (Fig. 3). Analogs described in this study are named with respect to their linker length; for example, cAuIB-2 refers to the cyclic AuIB analog with a two residue linker. Linkers were designed using functionally inert Ala and Gly residues, since these residues were not expected to interfere with receptor binding. Moreover, the linker has the potential to serve as an anchor point in future studies to attach various chemical moieties that could potentially enhance the pharmacokinetic properties of these molecules (17). In addition to the cyclic analogs, an *N*-terminal acetylated AuIB analog (*Ac*-AuIB) was also prepared to assess the requirement for an *N*-terminal charge.

An intramolecular native chemical ligation reaction was used to perform the N-to-C cyclization (9, 16). Conveniently, α-conotoxins contain multiple cysteine residues that give rise to four ligation sites. The least sterically hindered Gly-Cys site was selected and the linear thioester precursors were assembled accordingly (Fig. 4). An *S*-mercaptopropionamide thioester was used at the C-terminal and the linear thioester peptide precursors were conveniently assembled in parallel using a modified procedure with polypropylene tea bags (7), employing *tert*-butyloxycarbonyl *in situ* neutralization chemistry (42). After chain assembly, the peptides were cleaved from the resin using HF/*p*-cresol (9:1) to afford the crude linear thioester precursors. The identities and purity of the synthetic thioesters were confirmed by LC-MS analysis (Table 1), and the peptides were used in the subsequent cyclization step without further purification.

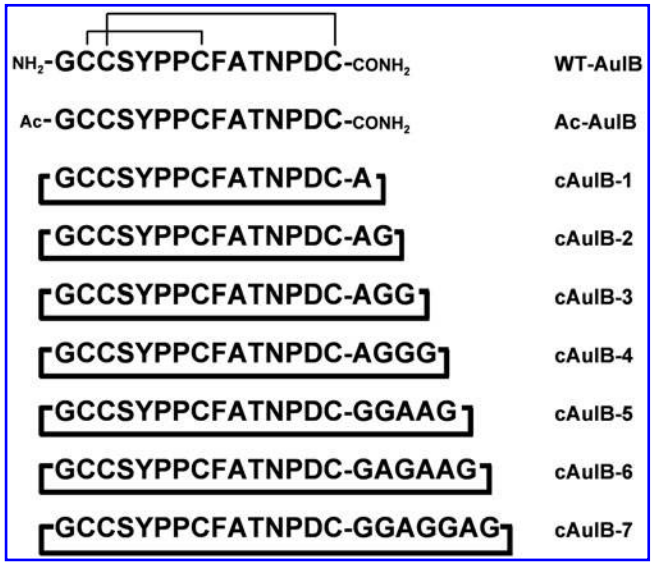

FIG. 3. Primary structures of α-conotoxin AuIB and its cyclic analogs. Seven N-to-C cyclic analogs of α-conotoxin AuIB that were prepared and used in this study.

Cyclization and random oxidation of the seven peptide thioesters was performed by stirring the crude linear thioester precursors in aqueous 0.1 M phosphate buffer, pH 8.2. Although reducing reagents such as thiophenol or 2-mercaptoethanesulfonic acid are often included in native chemical ligation reactions to catalyze the formation of more reactive thioesters (15), they were excluded in our synthesis to generate an oxidizing environment, which allows the *in situ* formation of the disulfide bonds. This one pot approach was advantageous, since isolation of the intermediates was not required. The cyclization was monitored by LC-MS (Table 1), and the N-to-C cyclization step occurred very rapidly (ca. <1 min) for all analogs. On the other hand, complete oxidation of the cysteine residues is much slower, ranging from 2 to 3 days with cAuIB-5, -6, and -7 requiring longer reaction times. Although cAuIB-1, -3, and -4 predominantly yielded one major disulfide bond isomer, cAuIB-2, -5, -6, and -7 formed one additional disulfide bond isomer (Fig. 5), which in the case of cAuIB-5, -6, and -7 were isolated to >95% purity by preparative RP-HPLC. However, the minor peaks of cAuIB-5, -6, and -7 were isolated in very small yields. Further, the two disulfide isomers of cAuIB-2 were not readily separated by RP-HPLC; thus, a directed disulfide bond forming strategy utilizing orthogonal cysteine protecting groups was required to obtain both isomers separately (Fig. 6). In this strategy, an additional iodine-mediated oxidation/deprotection of the Acm protected cysteine residues was used to form the second disulfide bond after the initial one pot cyclization/oxidation step. Subsequent purification by preparative HPLC yielded both isomers in high yield and purity, with each isomer exhibiting distinctly different analytical LC-MS retention times (Fig. 7). Co-injection of both globular and ribbon isomers of cAuIB-2 confirmed that both products were indeed different, allowing for the clear characterization of both isomers obtained using random oxidation strategy.

Determination of disulfide bond connectivity

To unambiguously confirm the disulfide bond connectivity of cAuIB-1, a modified reduction/alkylation strategy was used as previously described (11). The cyclic oxidized conotoxin was partially reduced with TCEP in acidic buffer to avoid scrambling of the disulfide bonds, followed by alkylation of the partially reduced peptide with *N*-ethylmaleimide. The cyclic peptide was then treated with α-chymotrypsin to cleave the cyclic backbone, followed by full reduction of the second disulfide bond using TCEP. The resulting linear peptide was sequenced using LC-MS/MS, which confirmed the location of the *N*-ethylmaleimide groups as being Cys3 and Cys8. Hence, cAuIB-1 was designated as the ribbon isomer.

We have previously used CD spectroscopy to characterize the secondary structure and assign the disulfide connectivity of α-conotoxins (Fig. 8) (2). Analogs that exhibit overlapping CD spectra can be assumed to share the same folding characteristics and disulfide bonding. As the cAuIB-2 globular and ribbon isomers were obtained separately using an orthogonal disulfide bond synthesis strategy, these were used to assist in identifying the disulfide connectivity of other isomers.

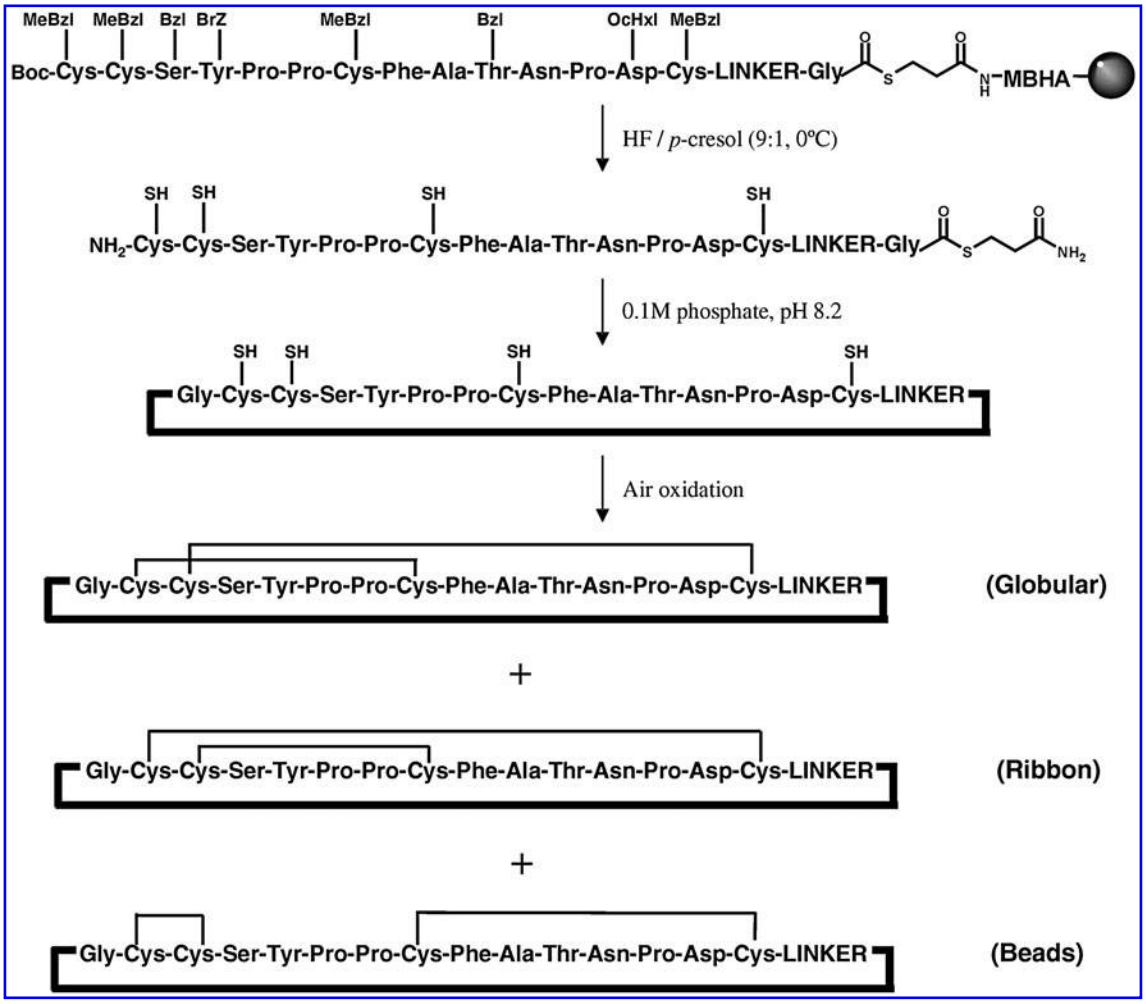

FIG. 4. Synthetic strategy for the preparation of cyclic analogs of α-conotoxin AuIB using one-pot cyclization/oxidation. Three possible disulfide isomers are available using nondirected oxidation. Acm, acetomidomethyl; BrZ, 2-bromobenzyloxycarbonyl; Bzl, benzyl; MBHA, 4-methylbenzhydrylamine; MeBzl, 4-methylbenzyl; OcHxl, O-cyclohexyl ester.

Table 1. Measured and Calculated Molecular Masses (Da) for Linear Thioester Precursors and Cyclic Oxidized AuIB Analogs After Liquid Chromatography Mass Spectrometry Analysis

	Molecular masses (Da)			
	Linear thioester precursor		*Cyclic oxidized product*	
Analog	*Found*	*Calculated*	*Found*	*Calculated*
WT-AuIB[a]	1575.6	1575.6	1571.6	1571.5
Ac-AuIB[a]	1617.6	1617.6	1613.6	1613.6
cAuIB-1	1734.6	1734.6	1625.6	1625.6
cAuIB-2	1791.6	1791.6	1682.7	1682.6
cAuIB-3	1848.4	1848.6	1739.6	1739.6
cAuIB-4	1905.6	1905.7	1796.8	1796.6
cAuIB-5	1976.8	1976.7	1867.6	1867.6
cAuIB-6	2047.8	2047.7	1938.8	1938.7
cAuIB-7	2090.6	2090.7	1981.8	1981.7

[a]Values are given for the linear reduced and linear oxidized conotoxins, respectively.
Ac, acetyl; WT, wild-type.

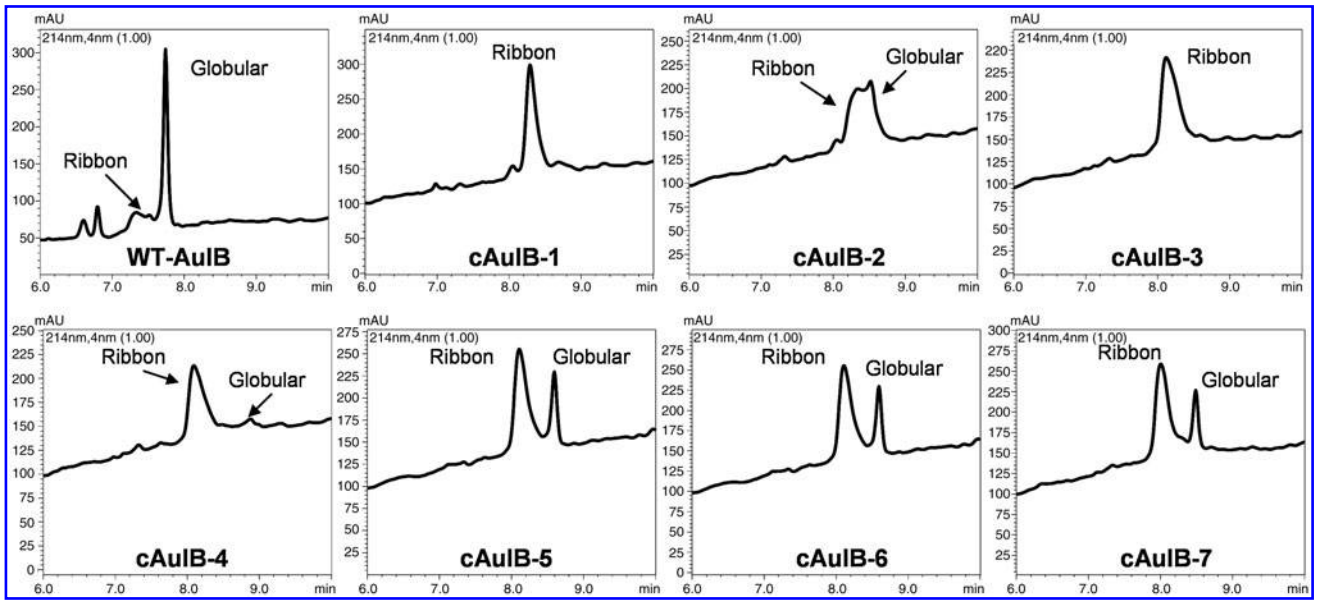

FIG. 5. Analytical liquid chromatography mass spectrometry traces of crude oxidized cyclic AuIB analogs. The presence of disulfide bond isomers is indicated. Each of the peaks corresponded to the calculated molecular mass (see Table 1).

Wild-type (WT)-AuIB exhibited a CD spectrum typical of a peptide with helical elements, with characteristic minima occurring at 222 nm (26). The cAuIB-2 globular isomer exhibited increased helical content compared to WT-AuIB, whereas the cAuIB-2 ribbon isomer displayed significantly less helical content, suggesting a more random structure. A similar trend was observed for each of the two isolated isomers of cAuIB-5, -6, and -7, allowing identification of each isolated product as either the globular or ribbon isomer (Fig. 8).

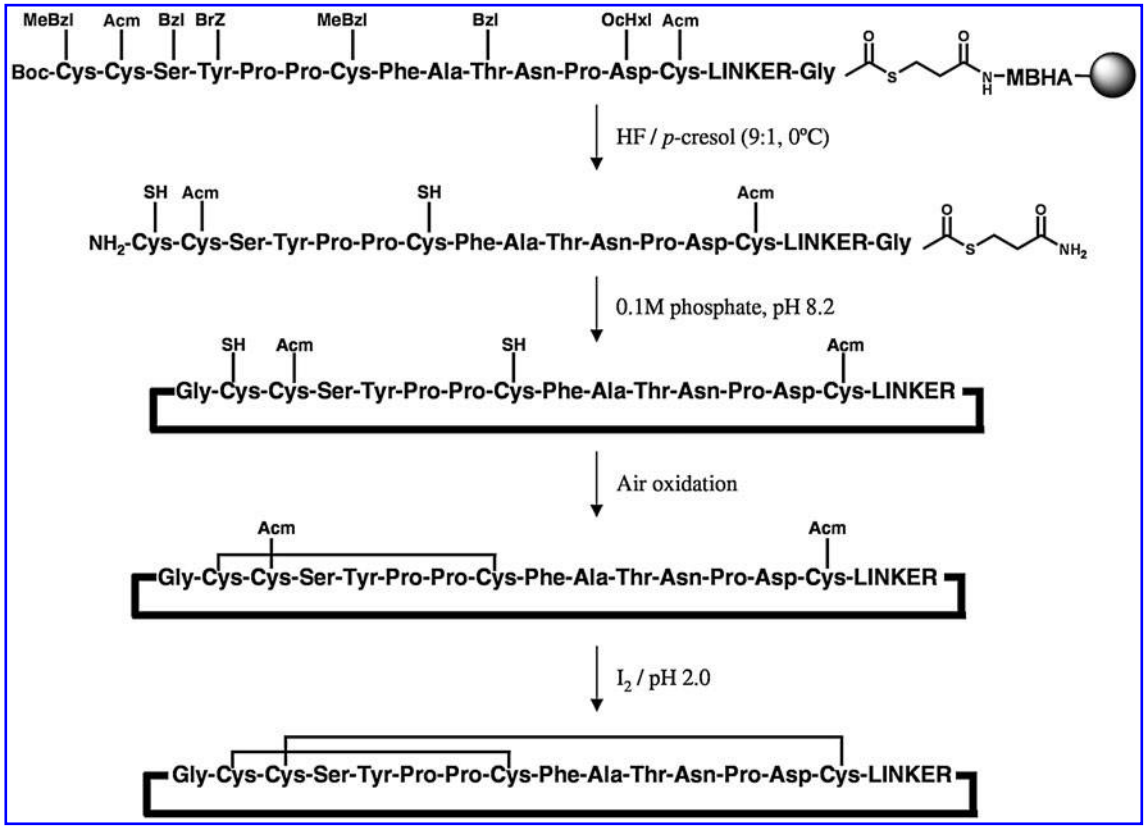

FIG. 6. Synthetic strategy for the preparation of cAuIB-2 using regioselective disulfide bond formation. The ribbon isomer was synthesized using essentially the same strategy, except that Cys8 was protected with Acm and Cys16 with 4-methylbenzyl.

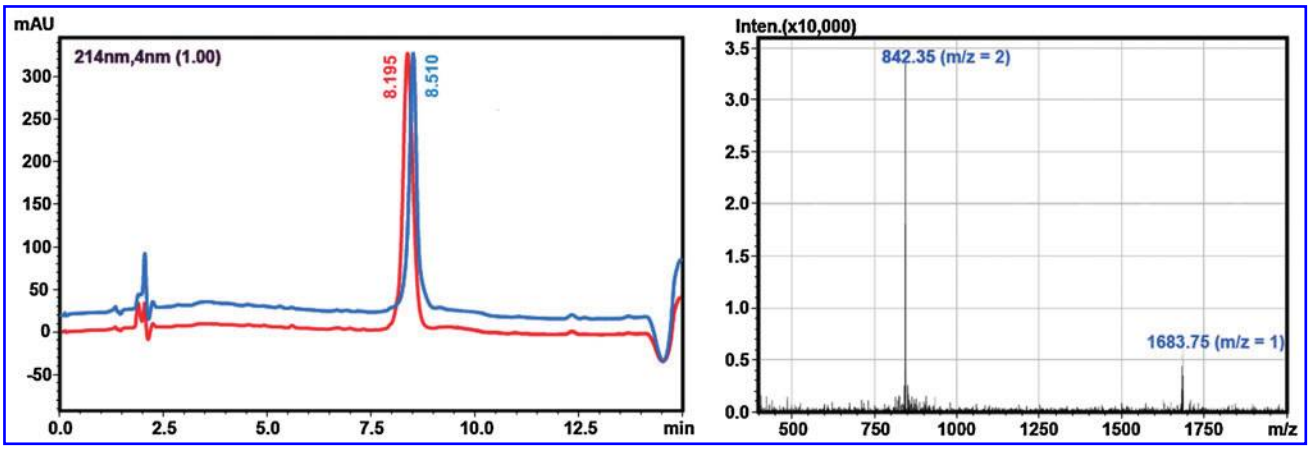

FIG. 7. Liquid chromatography mass spectrometry of cAuIB-2 globular and ribbon isomers. (*Left*) Overlay of LC traces for cAuIB-2 globular (blue) and ribbon isomer (red). LC retention times are indicated above the peaks. (*Right*) Mass spectrometry confirms the identity of cAuIB-2 ribbon as a fully oxidized cyclic analog. An identical spectrum was obtained for cAuIB-2 globular (data not shown). (For interpretation of the references to color in this figure legend, the reader is referred to the web version of this article at www.liebertonline.com/ars).

Pharmacological characterization

The functional properties of WT-AuIB and the AuIB analogs were characterized at three major neuronal nAChR subtypes, the $\alpha_3\beta_4$, α_7 and $\alpha_4\beta_2$, using two fluorescence-based screening assays (Ca^{2+}/Fluo-4 and FMP Blue assays) (Fig. 9). We and others have previously found that these fluorescence-based functional assays are in agreement with reported electrophysiological recordings (20, 46). WT-AuIB inhibited the $\alpha_3\beta_4$ nAChR signaling elicited by 100 n*M* epibatidine with an IC_{50} value of 9.1 μM, whereas it did not display any significant inhibition of $\alpha_4\beta_2$ and α_7 nAChR at concentrations up to 300 μM. The antagonist activity displayed by WT-AuIB at the $\alpha_3\beta_4$ nAChR in the assay was somewhat lower (~10-fold) than previously reported for the α-conotoxin at the nAChR expressed in *Xenopus* oocytes (37, 41). This difference is likely to arise from the different expression systems and assays used. *Ac*-AuIB exhibited slightly lower antagonist potency (17 μM) than WT-AuIB (Fig. 9). The cAuIB-2 globular isomer was the only cyclic analog that displayed activity at the $\alpha_3\beta_4$ nAChR, exhibiting an IC_{50} of 24 μM (Fig. 9), which represents a 2.6-fold decrease in inhibitory activity compared to WT-AuIB. In contrast, all cyclic ribbon isomer AuIB analogs displayed an $IC_{50} > 300\ \mu M$ at the $\alpha_3\beta_4$ nAChR subtype and therefore were defined as inactive. Further, none of the cyclic analogs displayed significant inhibitory activities at the α_7 or

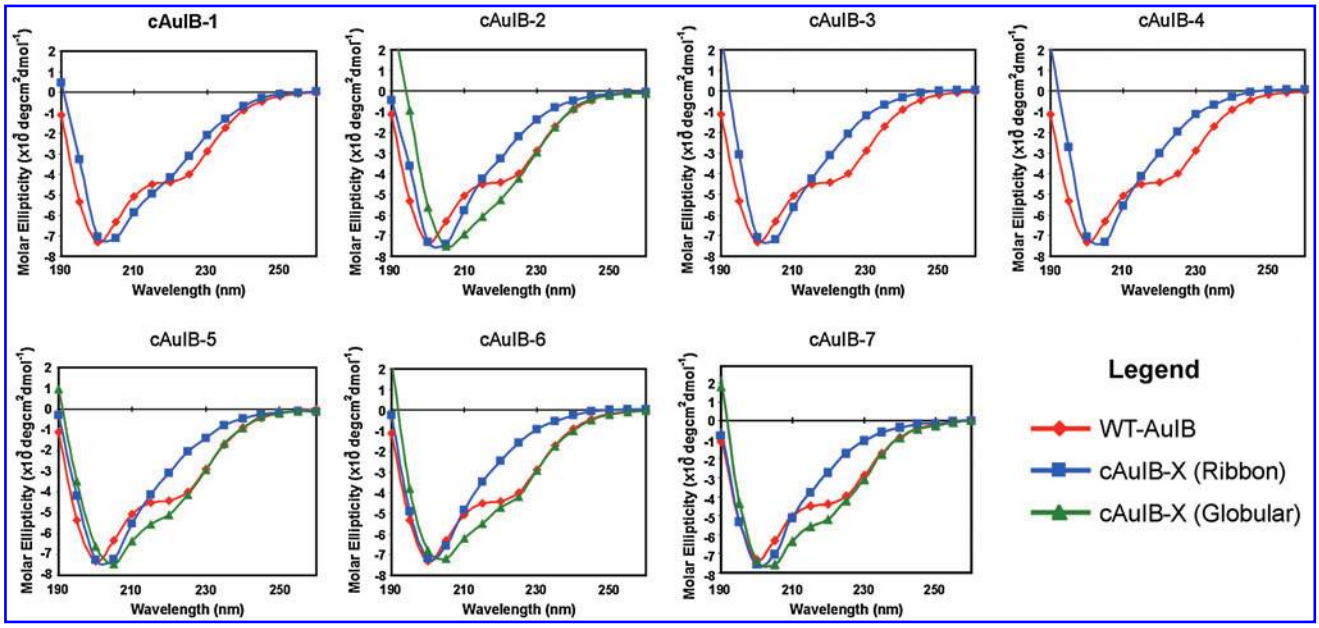

FIG. 8. Circular dichroism spectra of WT-AuIB compared with cyclic AuIB analogs. Red, WT-AuIB; Blue, cyclic ribbon isomer; Green, cyclic globular isomer. WT, wild-type. (For interpretation of the references to color in this figure legend, the reader is referred to the web version of this article at www.liebertonline.com/ars).

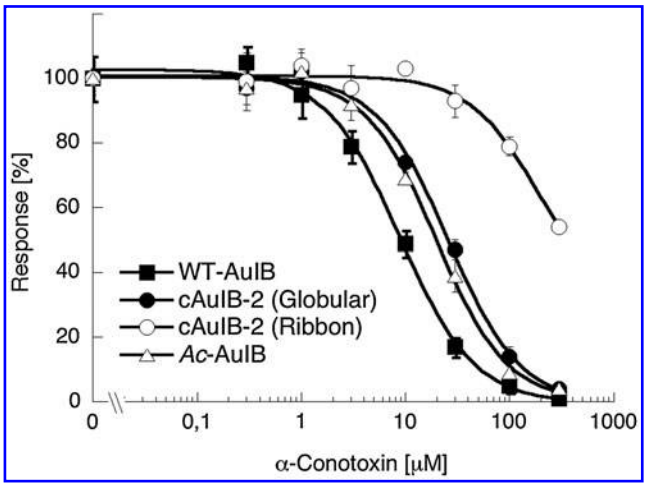

FIG. 9. Inhibition of $\alpha_3\beta_4$ nicotinic acetylcholine receptor signaling by native α-conotoxin AuIB, the globular and ribbon isomers of cAuIB-2 and Ac-AuIB. Concentration–inhibition curves for WT-AuIB, cAuIB-2 (globular), cAuIB-2 (ribbon), and Ac-AuIB at the r$\alpha_3\beta_4$-HEK293 cell line in the Ca^{2+}/Fluo-4 assay. The Ca^{2+}/Fluo-4 assay was performed as described in the Materials and Methods section using a final assay concentration of 200 n*M* epibatidine. The responses are given as differences in fluorescent units between peak fluorescence after agonist addition and the baseline fluorescence. The figure depicts data from a single representative experiment, and error bars are given as means ± standard deviation of duplicate determinations.

$\alpha_4\beta_2$ nAChR subtypes. As such, the cAuIB-2 globular isomer displays significant selectivity for the $\alpha_3\beta_4$ nAChR over the $\alpha_4\beta_2$ and α_7 subtypes.

Chymotrypsin stability

Enzymatic degradation was used to assess the stability of the ribbon isomer of each analog. AuIB contains a chymotrypsin cleavage site, specifically the C-terminal of Phe9; thus, its resistance to proteolysis can be used as a marker for peptide stability. Each analog was incubated with chymotrypsin at 37°C in 50 m*M* tris buffer at pH 7.4 and their hydrolysis monitored at various time intervals by LC-MS (Fig. 10). All of the cyclic analogs demonstrated an improved stability compared to WT-AuIB. However, the degree of stability correlates with linker length in the ribbon isomers, with cAuIB-3, -4, -5, -6, and -7 possessing significantly greater proteolytic resistance. Although cAuIB-1 (92% degradation after 48 h) exhibited no significant increase in stability compared to WT-AuIB (86% degradation after 48 h), the globular and ribbon isomers of cAuIB-2 both exhibited significantly increased stability compared to WT-AuIB; however, the globular isomer was found to be slightly less stable than the ribbon isomer (60% and 46% degradation after 48 h, respectively).

Discussion

The approval of Prialt by the U.S. Food and Drug Administration in 2004 as an intrathecal analgesic (39), together with the development of other conotoxin drug leads that are currently undergoing clinical trials for the treatment of neuropathic pain, has aroused much interest in the therapeutic potential of conotoxins for treating a wide range of neuropathological conditions (32). As such, structural templates that improve the pharmacokinetic properties of conotoxin drug leads are required to enhance their chemical and biological stability for use as *in vivo* probes and as drugs leads. Cyclization of conotoxins through their N- and C-termini has previously been shown to improve their stability under a range of biological conditions (6, 11, 34). Previous studies have shown that a shorter linker length linking the N- and C-termini can promote the formation of the ribbon disulfide bond isomer of α-conotoxins (6). Given that the ribbon isomer of α4/6-conotoxin AuIB has been shown to possess a 10-fold greater potency as an antagonist at native $\alpha_3\beta_4$ nAChRs than the globular isomer (18), we investigated the relationship between linker length on disulfide bond formation, conformation, stability, and biological activity of N-to-C cyclic analogs of AuIB at nAChRs.

Seven analogs that incorporated between one to seven amino acid linker units to link the N- and C-termini of AuIB were used in this study to investigate the impact of linker length on the formation of disulfide bond isomers, stability, and pharmacological activity. Parallel assembly of the linear thioester precursors using polypropylene tea bags allowed rapid access to multiple cyclic conotoxin analogs. A one-pot cyclization/oxidation utilizing an intermolecular native chemical ligation reaction was used to prepare the cyclic conotoxins as reported previously (6, 11), and the formation of disulfide bond isomers was monitored by LC-MS. Linker length was found to have a major influence on the formation of disulfide bond isomers, with a clear preference for the

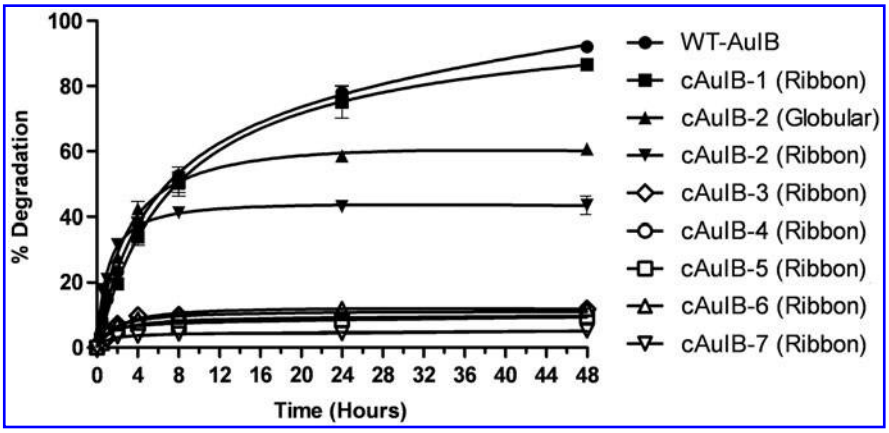

FIG. 10. α-Chymotrypsin degradation profile of WT-AuIB and its cyclic analogs. Error bars are given as means ± standard error of the mean of duplicate determinations.

formation of the ribbon isomer occurring in analogs with shorter linker lengths. However, the globular isomer was formed as a minor isomer in cAuIB-5, -6, and -7. The beads isomer was not observed for any of the analogs in this study. The globular isomer of cAuIB-2 formed along with the ribbon isomer in a 1:1 ratio, although these proved difficult to isolate by RP-HPLC. As such, both isomers of cAuIB-2 were synthesized separately using an orthogonal cysteine protecting group strategy, allowing sufficient quantities to be readily obtained in high yield and purity for pharmacological characterization.

CD spectroscopy of the ribbon and globular isomers of cAuIB-2, synthesized using regioselective control of disulfide bonds, allowed a convenient means for identifying different disulfide bond isomers obtained synthetically in the random oxidation strategy. Although the ribbon isomer of WT-AuIB has been found to possess greater activity at the native $\alpha_3\beta_4$ nAChRs (18), none of the cyclic ribbon isomers in this study were shown to possess any significant activity for the $\alpha_3\beta_4$ nAChR. This may be due to the restricted conformational mobility of the cyclic AuIB ribbon isomer analogs compared to the WT-AuIB ribbon isomer, which was previously found to possess a flexible backbone solution structure and would readily adopt the active conformation upon receptor binding (18). On the other hand, the cAuIB-2 globular isomer exhibited a moderate decrease in antagonist potency for the $\alpha_3\beta_4$ nAChR compared to WT-AuIB. This observation can be rationalized by absence of an *N*-terminal charge group, where the activity of *Ac*-AuIB was also lower for the $\alpha_3\beta_4$ nAChR than WT-AuIB. In this regard, the cAuIB-2 globular isomer exhibits comparable activity to *Ac*-AuIB. From a drug design perspective, the modest decrease in activity at the $\alpha_3\beta_4$ nAChR displayed by cAuIB-2 would most likely be offset by the significantly improved *in vivo* stability. Moreover, cAuIB-2 globular isomer was shown to be selective for this receptor subtype over the α_7 and $\alpha_4\beta_2$ subtypes, thus may find potential use as a stable probe for studying the role of $\alpha_3\beta_4$ nAChR in *in vivo* animal models.

Although cAuIB-2 was the only analog possessing the globular disulfide connectivity that was isolated in sufficient yield for pharmacological characterization, cAuIB-5, -6, and -7 globular isomers may exhibit similar pharmacological properties. In the case of cyclic analogs of α4/7-conotoxin MII, a linker of at least six residues was required to maintain structure and activity for the $\alpha_3\beta_2$ nAChR (11). We have found that in AuIB, a two-residue linker can yield analogs that possess a moderate decrease in activity compared to the native conotoxin. We speculate that this is the result of the restricted flexibility of the smaller *n* loop in AuIB, which has one less residue and may result in a tighter backbone fold compared to the 4/7 α-conotoxins. As such, precise fine-tuning of the linker unit is required for each different α-conotoxin loop spacing to minimize perturbing the three-dimensional structure (10). However, full characterization of cyclic AuIB analogs by NMR spectroscopy is required, which has been the subject of a separate investigation by Lovelace *et al.* (35).

Resistance to proteolytic cleavage by α-chymotrypsin was used as a model to determine the *in vitro* stability of the analogs. Although each of the cyclic analog ribbon isomers exhibited improved resistance to proteolytic cleavage by chymotrypsin, longer linker lengths (*i.e.*, cAuIB-3, -4, -5, -6, and -7) clearly demonstrate greater stability. In contrast, cAuIB-1 exhibited no significant increase in stability when compared to WT-AuIB (11). Although the ribbon isomer of WT-AuIB was not tested in the chymotrypsin stability assay, a comparison of the stability of the globular and ribbon isomers of cAuIB-2 shows that the globular isomer is moderately less stable to chymotrypsin degradation than its corresponding ribbon isomer. This result is somewhat surprising considering that the globular isomers of cyclic ImI analogs were previously shown to be more stable than the corresponding cyclic ribbon isomers (6). Nonetheless, when compared to WT-AuIB and cAuIB-1 (ribbon), the cAuIB-2 globular isomer exhibited significantly improved stability under the same conditions, with ~60% degradation occurring over 48 h.

In summary, we have demonstrated that N-to-C cyclization of α-conotoxin AuIB is a valuable means for achieving improved stability while maintaining biological activity and promises to be a useful strategy in the application of designing drug leads based on other novel α-conotoxin frameworks. Given the improved stability of the cAuIB-2 globular isomer compared to WT-AuIB, this analog could find use as a probe for studying the role of $\alpha_3\beta_4$ nAChRs in a number of *in vivo* experimental paradigms.

Acknowledgments

C.J.A. acknowledges a postdoctoral grant from the Drug Research Academy, The Faculty of Pharmaceutical Sciences, University of Copenhagen, and research funding from the State of Florida. A.A.J. was supported by the Lundbeck Foundation and the Danish Medical Research Council. Drs. Xiao, Kellar, Stitzel, and Feuerbach are thanked for their generous gifts of the nAChR-expressing cell lines.

Author Disclosure Statement

No competing financial interests exist.

References

1. Adessi C and Soto C. Converting a peptide into a drug: strategies to improve stability and bioavailability. *Curr Med Chem* 9: 963–978, 2002.
2. Armishaw C, Jensen AA, Balle T, Clark RJ, Harpsøe K, Skonberg C, Liljefors T, and Strømgaard K. The rational design of α-conotoxin analogues targeting α_7 nicotinic acetylcholine receptors: improved antagonistic activity by incorporation of proline derivatives. *J Biol Chem* 284: 9498–9512, 2009.
3. Armishaw CJ. Synthetic α-conotoxin mutants as probes for studying nicotinic acetylcholine receptors and in the development of novel drug leads. *Toxins* 2: 1470–1498, 2010.
4. Armishaw CJ and Alewood PF. Conotoxins as research tools and drug leads. *Curr Protein Pept Sci* 6: 221–240, 2005.
5. Armishaw CJ, Daly NL, Nevin ST, Adams DJ, Craik DJ, and Alewood PF. α-Selenoconotoxins: a new class of potent α7 neuronal nicotinic receptor antagonists. *J Biol Chem* 281: 14136–14143, 2006.
6. Armishaw CJ, Dutton JL, Craik DJ, and Alewood PF. Establishing regiocontrol of disulfide bond isomers of α-conotoxin ImI via the synthesis of N-to-C cyclic analogs. *Biopolymers* 94: 307–313, 2010.
7. Armishaw CJ, Singh N, Medina-Franco J, Clark RJ, Scott KCM, Houghten RA, and Jensen AA. A synthetic combinatorial strategy for developing α-conotoxin analogs as potent α7 nicotinic acetylcholine receptor antagonists. *J Biol Chem* 285: 1809–1821, 2010.

8. Azam L and McIntosh JM. Alpha-conotoxins as pharmacological probes of nicotinic acetylcholine receptors. *Acta Pharmacol Sin* 30: 771–783, 2009.
9. Camarero JA and Muir TW. Chemoselective backbone cyclisation of unprotected peptides. *J Chem Soc Chem Commun* 1369–1370, 1997.
10. Cho J-H, Mok KH, Olivera BM, McIntosh JM, Park K-H, and Han K-H. Nuclear magnetic resonance solution conformation of α-conotoxin AuIB, an α3β4 subtype-selective neuronal nicotinic acetylcholine receptor antagonist. *J Biol Chem* 275: 8680–8685, 2000.
11. Clark RJ, Fischer H, Dempster L, Daly NL, Rosengren KJ, Nevin ST, Meunier FA, Adams DJ, and Craik DJ. Engineering stable peptide toxins by means of backbone cyclization: stabilization of the α-conotoxin MII. *Proc Natl Acad Sci USA* 102: 13767–13772, 2005.
12. Clark RJ, Jensen J, Nevin ST, Callaghan BP, Adams DJ, and Craik DJ. The engineering of an orally active conotoxin for the treatment of neuropathic pain. *Angew Chem* 2010 [Epub ahead of print].
13. Colgrave ML and Craik DJ. Thermal, chemical, and enzymatic stability of the cyclotide Kalata B1: the importance of the cyclic cysteine knot. *Biochemistry* 43: 5965–5975, 2004.
14. Craik DJ. Seamless proteins tie up their loose ends. *Science* 311: 1563–1564, 2006.
15. Dawson PE, Churchill MJ, Ghadiri R, and Kent SBH. Modulation of reactivity in native chemical ligation through use of thiol additives. *J Am Chem Soc* 119: 4325–4329, 1997.
16. Dawson PE, Muir TW, Clark-Lewis I, and Kent SBH. Synthesis of proteins by chemical ligation. *Science* 266: 776–779, 1994.
17. Dekan Z, Paczkowski FA, Lewis RJ, and Alewood PF. Synthesis and *in vitro* biological activity of cyclic lipophilic χ-conotoxin MrIA analogues. *Int J Pept Res Ther* 13: 307–312, 2007.
18. Dutton JL, Bansal PS, Hogg RC, Adams DJ, Alewood PF, and Craik DJ. A new level of conotoxin diversity, a non-native disulfide bond connectivity in α-conotoxin AuIB reduces structural definition but increases biological activity. *J Biol Chem* 277: 48849–48857, 2002.
19. Dutton JL and Craik DJ. α-Conotoxins: nicotinic acetylcholine receptor antagonists as pharmacological tools and potential drug leads. *Curr Med Chem* 8: 327–344, 2001.
20. Feuerbach D, Lingenhöhl K, Dobbins P, Mosbacher J, Corbett N, Nozulak J, and Hoyer D. Coupling of human nicotinic acetylcholine receptors α7 to calcium channels in GH3 cells. *Neuropharmacology* 48: 215–227, 2005.
21. Gehrmann J, Alewood PF, and Craik DJ. Structure determination of the three disulfide bond isomers of α-conotoxin GI: a model for the role of disulfide bonds in structural stability. *J Mol Biol* 278: 401–415, 1998.
22. Gilon C, Halle D, Chorev M, Selinger Z, and Byk G. Backbone cyclization: a new method for conferring conformational constraint of peptides. *Biopolymers* 31: 745–750, 1991.
23. Glick SD, Maisonneuve IM, and Kitchen BA. Modulation of nicotine self-administration in rates by combination therapy with agents blocking α3β4 nicotinic receptors. *Eur J Pharmacol* 448: 185–191, 2002.
24. Houghten RA. General-method for the rapid solid-phase synthesis of large numbers of peptides—specificity of antigen-antibody interaction at the level of individual amino-acids. *Proc Natl Acad Sci USA* 82: 5131–5135, 1985.
25. Jensen AA, Frølund B, Liljefors T, and Krogsgaard-Larsen P. Neuronal nicotinic acetylcholine receptors: structural revelations, target identifications and therapeutic inspirations. *J Med Chem* 48: 4705–4744, 2005.
26. Johnson WC Jr. Protein secondary structure and circular dichroism: a practical guide. *Proteins: Struct Funct Genet* 7: 205–214, 1990.
27. Karadsheh MS, Shah MS, Tang X, MacDonald RL, and Stitzel JA. Functional characterization of mouse α4β2 nicotinic acetylcholine receptors stably expressed in HEK293T cells. *J Neurochem* 91: 1138–1150, 2004.
28. Kessler H. Conformation and biological activity of cyclic peptides. *Angew Chem Int Ed* 21: 512–523, 1982.
29. Lewis RJ. Conotoxins as selective inhibitors of neuronal ion channels, receptors and transporters. *IUMBM Life* 56: 89–93, 2004.
30. Lewis RJ and Garcia ML. Therapeutic potential of venom peptides. *Nat Rev Drug Discov* 2: 790–802, 2003.
31. Lien S and Lowman HB. Therapeutic peptides. *Trends Biotechnol* 21: 556–562, 2003.
32. Livett B, Gayler KR, and Khalil Z. Drugs from the sea: conopeptides as potential therapeutics. *Curr Med Chem* 11: 1715–1723, 2004.
33. Livett BG, Sandall DW, Keays D, Down J, Gayler KR, Satkunanathan N, and Khalil Z. Therapeutic applications of conotoxins that target the neuronal nicotinic acetylcholine receptor. *Toxicon* 48: 810–829, 2006.
34. Lovelace ES, Armishaw CJ, Colgrave ML, Wahlstrom ME, Alewood PF, Daly NL, and Craik DJ. Cyclic MrIA: a stable and potent cyclic conotoxin with a novel topological fold that targets the norepinephrine transporter. *J Med Chem* 49: 6561–6568, 2006.
35. Lovelace ES, Gunasekera S, Alvarmo C, Clark RJ, Nevin ST, Grishin AA, Adams DJ, Craik DJ, and Daly NL. Stabilization of α-conotoxin AuIB: influences of disulfide connectivity and backbone cyclization. *Antioxid Redox Signal* 14: 87–95, 2011.
36. Lukas RJ, Changeux J-P, Le Novere N, Albuquerque EX, Balfour DJK, Berg DK, Bertrand D, Chiappinelli VA, Clarke PBS, Collins AC, Dani JA, Grady SR, Kellar KJ, Lindstrom JM, Marks MJ, Quik M, Taylor PW, and Wonnacott S. International union of pharmacology. XX. Current status of the nomenclature for nicotinic acetylcholine receptors and their subunits. *Pharmacol Rev* 51: 397–401, 1999.
37. Luo S, Kulak JM, Cartier GE, Jacobsen RB, Yoshikami D, Olivera BM, and McIntosh JM. α-Conotoxin AuIB selectively blocks α3β4 nicotinic acetylcholine receptors and nicotine-evoked norepinephrine release. *J Neurosci* 18: 8571–8579, 1998.
38. Marx UC, Daly NL, and Craik DJ. NMR of conotoxins: structural features and an analysis of chemical shifts of post-translationally modified amino acids. *Magn Reson Chem* 44: S41–S50, 2006.
39. Miljanich GP. Ziconotide: neuronal calcium channel blocker for treating severe chronic pain. *Curr Med Chem* 11: 3029–3040, 2004.
40. Myers RA, Cruz LJ, Rivier JE, and Olivera BM. Conus peptides as chemical probes for receptors and ion channels. *Chem Rev* 93: 1923–1936, 1993.
41. Nicke A, Samochocki M, Loughnan ML, Bansal PS, Maelicke A, and Lewis RJ. α-Conotoxins EpI and AuIB switch subtype selectivity and activity in native versus recombinant nicotinic acetylcholine receptors. *FEBS Lett* 554: 219–223, 2004.
42. Schnölzer M, Alewood P, Jones A, Alewood D, and Kent SBH. *In Situ* neutralization in boc-chemistry solid phase peptide synthesis. *Int J Pept Res Ther* 13: 31–44, 2007.

43. Struthers AM, Wilkinson JL, Dwoskin LP, Crooks PA, and Bevins RA. Mecamylamine, dihydro-β-erythroidine, and dextromethorphan block conditioned responding evoked by the conditional stimulus effects of nicotine. *Pharmacol Biochem Behav* 94: 319–328, 2009.
44. Taly A, Corringer P-J, Guedin D, Lestage P, and Changeux JP. Nicotine receptors: allosteric transitions and therapuetic targets in the nervous system. *Nat Rev Drug Discov* 8: 733–750, 2009.
45. Terlau H and Olivera BM. Conus venoms: a rich source of novel ion channel-targeted peptides. *Physiol Rev* 84: 41–68, 2004.
46. Xiao Y, Meyer EL, Thompson JM, Surin A, Wroblewski J, and Kellar KJ. Rat α3/β4 subtype of neuronal nicotinic acetylcholine receptor stably expressed in a transfected cell line: pharmacology of ligand binding and function. *Mol Pharmacol* 54: 322–333, 1998.

Address correspondence to:
Dr. Christopher J. Armishaw
Torrey Pines Institute for Molecular Studies
11350 SW Village Pkwy
Port St. Lucie, FL 34957

E-mail: carmishaw@tpims.org

Prof. Kristian Strømgaard
Department of Medicinal Chemistry
Faculty of Pharmaceutical Sciences
University of Copenhagen
Universitetsparken 2
Copenhagen Ø, DK-2100
Denmark

E-mail: krst@farma.ku.dk

Date of first submission to ARS Central, July 6, 2010; date of acceptance, July 18, 2010.

Abbreviations Used

Ac = acetyl
Acm = acetomidomethyl
BrZ = 2-bromo-benzyloxycarbonyl
Bzl = benzyl
CD = circular dichroism
FMP = FLIPR™ Membrane Potential
LC-MS = liquid chromatography mass spectrometry
MBHA = 4-methylbenzhydrylamine
MeBzl = 4-methylbenzyl
nAChR = nicotinic acetylcholine receptor
OcHxl = *O*-cyclohexyl ester
RP-HPLC = reversed phase high performance liquid chromatography
TCEP = *tris*-(2-carboxyethyl)phosphine hydrochloride
TFA = trifluoroacetic acid
WT = wild-type

This article has been cited by:

1. Christina I Schroeder, David J Craik. 2012. Therapeutic potential of conopeptides. *Future Medicinal Chemistry* **4**:10, 1243-1255. [CrossRef]
2. Reena Halai, Brid Callaghan, Norelle L Daly, Richard J Clark, David J. Adams, David J Craik. 2011. Effects of cyclization on stability, structure and activity of #-conotoxin RgIA at the #9#10 nicotinic acetylcholine receptor and GABA_B receptor. *Journal of Medicinal Chemistry* 110902150200066. [CrossRef]
3. David J. Craik . 2011. The Folding of Disulfide-Rich Proteins. *Antioxidants & Redox Signaling* **14**:1, 61-64. [Abstract] [Full Text HTML] [Full Text PDF] [Full Text PDF with Links]